Stagnation line approximation for ablation thermochemistry

Julien de Mûelenaere[*]

Aeronautics and Aerospace Department, von Karman Institute for Fluid Dynamics, Belgium

Jean Lachaud[†]

UARC/UC Santa Cruz, Moffet Field, CA

Nagi N. Mansour[‡]

NASA Ames Research Center, Moffet Field, CA

Thierry E. Magin[§]

Aeronautics and Aerospace Department, von Karman Institute for Fluid Dynamics, Belgium

A stagnation line formulation is derived for ablation thermochemistry and used to solve for the distribution of species, density, and enthalpy in a chemically active boundary layer. The formulation is used to compute B'-tables that include the mass diffusion terms and the effects of wall blowing on the boundary layer. This formulation avoids the need of a blowing correction used in material response modeling. B'-tables are commonly used in ablative material response modeling to determine the consumption rate of material at the surface, B'_c, as a function of pyrolysis gas mass flux, B'_g, temperature and pressure. A thin control volume is considered where conservation of mass, equilibrium chemistry, and the transfer potential approximation to the diffusion transport terms are used to determine B'-tables as a function of temperature and pressure. The sensitivity of the tables to using equilibrium chemistry coefficients from JANAF fits, Gurvich fits and a rigid rotor/harmonic oscillator approximation is investigated. Little effect of the fits is found at temperatures below 2,250K. However, important differences at high temperatures have been identified. Differences at high temperatures were also found between B'-tables derived using the simplest mass transfer approximation and tables derived without the need to approximate the diffusion transport terms. This implies that estimates of the recession rate of ablative material in high enthalpy environments are sensitive to the approach used to build B'-tables.

I.   Introduction

Exploration beyond low-earth orbit and sample-return missions require reentering the atmosphere at speeds above 10 km/s. In planning missions to planets with atmospheres, optimization of the mass of the fuel and the mass of the heat shield often results in high speed atmospheric entries. To achieve these missions, the mission designer relies on the availability of ablative materials. These specially designed materials harness interactions between the flow environment and the surface (gas-surface interactions) to protect the payload. They are designed to be an insulator that rejects heat by re-radiating and blowing the majority of the incident heat back into the environment. In this process, ablative materials lose mass and their surface recesses. A crucial tool in the design process of a thermal protection system is therefore a model that predicts the required thickness for the payload to remain protected during atmospheric entry.

A common strategy, first proposed by Kendall et al.[1] in 1968, is to run material and flow codes decoupled and approximate their interactions through the use of heat and mass transfer coefficients. The flow

---

[*]Ph.D. Candidate, Aeronautics and Aerospace Department, von Karman Institute for Fluid Dynamics, Chaussée de Waterloo 72, 1640 Rhode-Saint-Genèse, Belgium

[†]Associate Scientist, AIAA senior member.

[‡]Chief Scientist for Modeling and Simulation, Space Technology Division. AIAA Associate fellow.

[§]Assistant Professor, Aeronautics and Aerospace Department, von Karman Institute for Fluid Dynamics, Chaussée de Waterloo 72, 1640 Rhode-Saint-Genèse, Belgium

American Institute of Aeronautics and Astronautics

environment code uses "cold-wall" boundary conditions, i.e. independent of the material response code, but provides the heat transfer coefficients, density, pressure, enthalpy, and species mass fractions at the boundary layer edge. The material code, on the other hand, estimates the surface recession rate through the use of tables. Kendall et al.[1] generated non-dimensional pyrolysis-gas mass flux and char consumption rate, B'_g and B'_c, tables (commonly referred to as B'-tables) by considering a thin control volume where the gas-surface interactions occur and where mass balance and equilibrium chemistry are satisfied. To obtain the diffusive transport terms that appear in the mass conservation equation, they used heat and mass transfer coefficients to relate the boundary layer edge quantities to the quantities in the control volume. Because of the efficiency of this strategy, it is still followed today.[2]

A weakness in this strategy is in the model of mass transport due to diffusion into the control volume. In addition, we expect that blowing the byproducts of the ablation process into the boundary layer will change the conditions in the boundary layer. MacLean et al.[3] and Gnoffo et al.[4] have shown that coupling the byproducts of ablation to the fluid code has an important impact on the flow environment.

While flow solvers have now been developed[3,4] that can bypass the use of B'-tables, efforts to tightly couple them to an in-depth material response solver are still work-in-progress. These efforts will result in large codes that are designed for applications that require massive parallel computing capability. However, there is a need for approximate solvers that can be used on a personal computer. In this paper, we develop a stagnation line formulation and use it to test one of the approximations for the diffusion mass transport suggested by Kendall et al.[1] We solve for the distribution of species, density, and enthalpy in the boundary layer given conditions at the boundary layer edge. This new capability enables us to produce B'-tables that account for diffusion and blowing into the boundary layer, and we compare these to B'-tables generated using the approximations.

The present paper is organized as follows: in section (II), the thin control volume approach of Kendall et al.[1] is revisited. Their simplest approximation is used to compare B'-tables generated using CEA[5] fits, JANAF[11] fits, and a rigid rotor/harmonic oscillator approximation to the thermodynamics.[6] In section (III), the stagnation line approximation is derived without the use of self similar coordinates to represent the boundary layer at the stagnation line. In section (IV), a new approach for the generation of B'-tables is developed by means of coupling the thin control volume formulation to the stagnation line solution. Summary and conclusions are presented in section (V).

II.   Thin Control Volume

The B'-tables are built based on conservation of mass and equilibrium chemistry. They are essentially a means to impose a boundary condition on an ablation code without having to couple the flow environment. To compute the equilibrium mixture, the species equilibrium constants (functions of the Gibbs free energy) are obtained from fits to the species thermodynamic properties. Modifications to the equilibrium chemistry assumption may be added to account for heterogeneous finite-rate chemistry or material failure;[1] unfortunately, this methodology relies on rates and ablation mechanisms that are not well understood[7] and will not be considered in this paper. In a companion paper, the heterogeneous finite-rate chemistry of a carbon preform is analyzed.[8] In this section, we revisit the derivation of the open control volume[1] formulation to familiarize the reader with the details of the formulation and our choice of approximation for the diffusion transport terms.
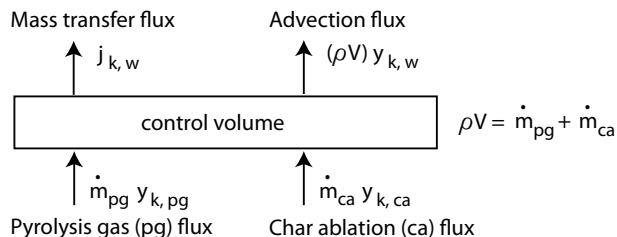
Figure 1. Mass fluxes and compositions at the wall

American Institute of Aeronautics and Astronautics

A.   Mass Balance

We start with a *Thin Control Volume* (*TCV*), as shown in Fig. 1, that encloses the gas surface interface in the moving reference frame of the surface. We assume that: (1) the surface is chemically active with carbon char (C(gr)), assumed in equilibrium with the gas species, reacting with oxygen and sublimating; (2) the pyrolysis gas products and the gas from the flow environment get transported into the control volume at a rate slow compared to the chemistry time-scale, thus enabling equilibrium to be established for the mixture within the control volume. We further assume no accumulation of gas in the *TCV*. The mass balance of the elements in the control volume is given by,

$$\dot{m}_{pg} y_{k,pg} + \dot{m}_{ca} y_{k,ca} = (\rho V)_w y_{k,w} + j_{k,w} \tag{1}$$

where $y_{k,pg}$, $y_{k,ca}$, and $y_{k,w}$ are the mass fraction of the elements in the gas, the char, and the mixture, respectively; $\dot{m}_{pg}$ and $\dot{m}_{ca}$ are the pyrolysis gas mass flux and the char mass consumption rate $[kg\,m^{-2}s^{-1}]$; ρ is the density of the mixture $[kg/m^3]$; V is the velocity of the gas mixture, $[m/s]$; and $j_{k,w}$ is the diffusion flux of the elements of the mixture, $[kg\,m^{-2}s^{-1})]$ given by,

$$j_{k,w} = \sum_i \nu_k^i \frac{M_k}{M_i} J_{yi,w} \tag{2}$$

where ν_k^i are stoichiometric coefficients that are defined in Eq. 6, M_i is the molar mass of species i, and $J_{yi,w}$ is the mixture species diffusion flux.

By summing over the elements k in Eq. 1, we get the total mass conservation equation,

$$\dot{m}_{pg} + \dot{m}_{ca} = (\rho V)_w \tag{3}$$

Kendall et al.[1] considered several approximations to the species diffusion flux. The simplest of these approximations and the one we will adopt here is the transfer potential method that assumes equal mass diffusion coefficients for all species in the mixture:

$$j_{k,w} = \rho_e u_e C_M \left(y_{k,w} - y_{k,e} \right) \tag{4}$$

where ρ_e is the density of the gas at the boundary layer edge, u_e is the velocity at the boundary edge, $[m/s]$, and C_M is the Stanton number for mass transfer. Corrections to account for unequal diffusion coefficients have been proposed by Kendall et al. but are not currently used.[9]

By substituting equations (3) and (4) into (1) and rearranging terms, we get the elemental composition of the mixture,

$$y_{k,w}(\dot{m}_{ca}) = \frac{\dot{m}_{pg} y_{k,pg} + \dot{m}_{ca} y_{k,ca} + \rho_e u_e C_M y_{k,e}}{\dot{m}_{pg} + \dot{m}_{ca} + \rho_e u_e C_M} \tag{5}$$

The mass fractions of the elements in the mixture, $y_{k,w}$, and the ablation mass loss rate, $\dot{m}_{ca}$, are the unknowns that we need to determine. These represent $n_c + 1$ unknowns, where n_c is the number of elements.

B.   Chemistry for heterogeneous mixtures

The convention we will follow starts by expressing the formation reactions for n_s species as,[9]

$$\sum_k \nu_k^j N_k \rightarrow \nu_j^j N_j \tag{6}$$

where N_k represents base species for the elements in the system, ν_k^j are the stoichiometric coefficients of the formation reactions, and N_j is the gaseous product species formed by the reaction.

1.   Gaseous mixture

To compute the equilibrium composition of a gaseous mixture composed of n_s different chemical species, n_s independent equations are needed. We have $n_r = n_s - n_c$ independent equations obtained from the equilibrium of the formation reactions, Eq. 6, where n_c is the number of *base species* that are elements. Because of the adopted convention for the species formation reactions, n_c species formation reactions are trivial.

Equilibrium of the chemical reactions

Assuming that the species of the mixture are in chemical equilibrium, n_r equations are obtained from the definition of the equilibrium constants,

$$K_j = \left[\frac{Products}{Reactants}\right] = \frac{x_j^{\nu_j^j}}{\prod_k x_k^{\nu_k^j}} \tag{7}$$

From the above convention, the equilibrium constants are given by

$$\ln K_j\left(T,p\right) = -\frac{1}{RT}\left(\nu_j^j g_j\left(T,p_{ref}\right) - \sum_k \nu_k^j g_k\left(T,p_{ref}\right)\right) - \ln\left(\frac{p}{p_{ref}}\right)\left(\nu_j^j - \sum_k \nu_k^j\right) \tag{8}$$

where $g_i = h_i - Ts_i$ is the species Gibbs free energy and p_{ref} is a reference pressure.

Mass conservation of the elements

The remaining, $n_c = n_s - n_r$, equations are obtained from the mass conservation of the nuclei,

$$\nu_k^k x_k + \sum_j \nu_k^j x_j = \nu_k^k M \frac{y_{k,w}}{M_k} \tag{9}$$

where M, the gas-phase average molecular weight ($M = \sum_i M_i x_i$), is an additional unknown in the system. At this point, we have n_s equations for $n_s + 2$ unknowns. We seek two additional relations.

Mole-Fraction definition

By definition, the mole fractions sum to one. This provides an additional equation:

$$\sum_i x_i = 1 \tag{10}$$

To summarize, for a gaseous mixture, the system of $n_s + 1$ independent equations reads:

$$\begin{cases} \nu_k^k x_k + \sum_j \nu_k^j x_j &=& \nu_k^k M y_{k,w}(\dot{m}_{ca})/M_k \\ \sum_i x_i &=& 1 \\ \nu_j^j \ln x_j - \sum_k \nu_k^j \ln x_k &=& \ln K_j \end{cases} \tag{11}$$

The remaining constraint is obtained by considering the condensed phase reaction.

2. Condensed phase species chemistry

In the presence of solid reacting species (as is the case for ablating materials), solid species are added to the system. Therefore, heterogeneous equilibrium reactions are needed to close the system. Our current interest is in carbon-based materials, therefore, we will consider a char composed of a single element, $C(gr)$, formed by the following elementary reaction

$$C \rightarrow C(gr) \tag{12}$$
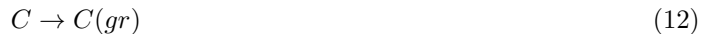
where C is carbon gas. In the case of ablative materials, it is assumed that the solid behaves as an infinite source of condensed species when present. Therefore, the activity of the solid (or its mole fraction), is taken equal to one, $x_{C(gr)} = 1$, in heterogeneous equilibrium reactions (it is equal to zero when not present). The following system is added to the gaseous species system,

$$\begin{cases} x_{C(gr)} &=& 1 \\ -\ln x_C &=& \ln K_{C(gr)} \end{cases} \tag{13}$$

American Institute of Aeronautics and Astronautics

The equilibrium constant for condensed-phase species reads:

$$\ln K_{C(gr)}(T,p) = -\frac{1}{RT}\left(g_{C(gr)}(T) - g_C(T,p_{ref})\right) + \ln\left(\frac{p}{p_{ref}}\right) \qquad (14)$$

Fits for the Gibbs free energy of carbon graphite $g_{C(gr)}(T)$ can be found in the literature.[6]

3. Complete System

The complete homogeneous/heterogeneous equilibrium chemistry system coupled to mass transfer reads

$$\begin{cases} \nu_k^k x_k + \sum_j \nu_k^j x_j &=& \nu_k^k M y_{k,w}(\dot{m}_{ca})/M_k \\ \sum_i x_i &=& 1 \\ -\ln x_C &=& \ln K_{C(gr)} \\ \nu_j^j \ln x_j - \sum_k \nu_k^j \ln x_k &=& \ln K_j \end{cases} \qquad (15)$$

The system is closed: we have $(n_s + 2)$ unknowns and $(n_s + 2)$ equations; M and $\dot{m}_{ca}$ are 2 additional unknowns to the mole fractions of the mixture . The system is quadratic in these unknown quantities and an iterative procedure is used to solve it. It is interesting to note that only gaseous species mole fractions appear in the system. This is due to the fact that the mole fraction of gaseous carbon C is fixed by the heterogeneous equilibrium reaction $-\ln x_C = \ln K_{C(gr)}$ as long as graphite is present in the mixture. Carbon gas is carried out of the wall by diffusion and convection simultaneously, causing ablation.

Two intensive variables need to be fixed to solve the equilibrium chemistry problem. We choose the pressure and temperature as our state variables, because they are the available variables when coupling to a material response code. The input variables are $y_{k,pg}$, $\dot{m}_{pg}$ (given by the material response code), $\rho_e u_e C_M$, and $y_{k,e}$ (e for edge; these depend on the surrounding atmposphere), $y_{k,ca}$, T_w, and p_w. The current code implementation provides $\dot{m}_{ca}$ that is needed to compute the recession rate of the surface:

$$rr = \frac{\dot{m}_{ca}}{\rho_{ca}} = \frac{[kg/m^2/s]}{[kg/m^3]} \qquad (16)$$

where ρ_{ca} is the density of the charred ablative material.

The computation also provides the species composition x_i, from which the total enthalpy of the gas in the control volume, h_w, can be evaluated.

The formulation has been implemented in the existing code MUTATION.[10] We refer to the code that implements the algorithm to solve the system given by Eq. 15 as MUTATION-B. The current code may be used to generate pre-computed B'-tables. It provides the dimensionless ablation mass-loss rate, $B'c = \dot{m}_{ca}/\rho_e u_e C_M$, and the wall enthalpy as a function of pressure, temperature, and the dimensionless pyrolysis-gas flow rate $B'_g = \dot{m}_{pg}/\rho_e u_e C_M$.

C. Representative B'-tables for carbon fibers with pyrolysis gas from phenolic

We have outlined a procedure where given $\dot{m}_{pg}$, T_w and p_w, and $\rho_e u_e C_M$, we can compute $\dot{m}_{ca}$. Kendall et al.[1] observed that by normalizing Eq. 5 using $\rho_e u_e C_M$, the system becomes independent of the conditions at the boundary layer edge and the Stanton number. Eq. 5 was then normalized and rearranged to read,

$$y_{k,w} = \frac{B'_g y_{k,pg} + B'_c y_{k,ca} + y_{k,e}}{B'_g + B'_c + 1} \qquad (17)$$

Rewriting the above equation in terms of B'_c, we get,

$$B'_c = -\frac{B'_g(y_{k,pg} - y_{k,w}) + (y_{k,e} - y_{k,w})}{(y_{k,ca} - y_{k,w})} \qquad (18)$$

where $B'_g = \dot{m}_{pg}/\rho_e u_e C_M$ and $B'_c = \dot{m}_{ca}/\rho_e u_e C_M$. We recall that B'_c is the key quantity extracted from the B'-tables to compute the recession rate.

MUTATION-B developed for the system of equations outlined in the previous sections was used to study an ex-phenolic pyrolysis-gas mixture in air. Starting from a mixture of about 150 species (corresponding to

American Institute of Aeronautics and Astronautics

the species available in the JANAF[11] and Gurvich[6] tables containing C, H, O, N), we removed species from the mixture and checked that the B' obtained did not change in the temperature range of interest, $500K$ - $4000K$. With 4 elements (C, H, O, and N) included, we were able to reduce the mixture to 19 representative species: C, H, O, N, CH, CH_4, CO, CO_2, CN, C_2, C_2H, C_2H_2, C_3, C_4, C_5, HCN, H_2, H_2O, N_2.
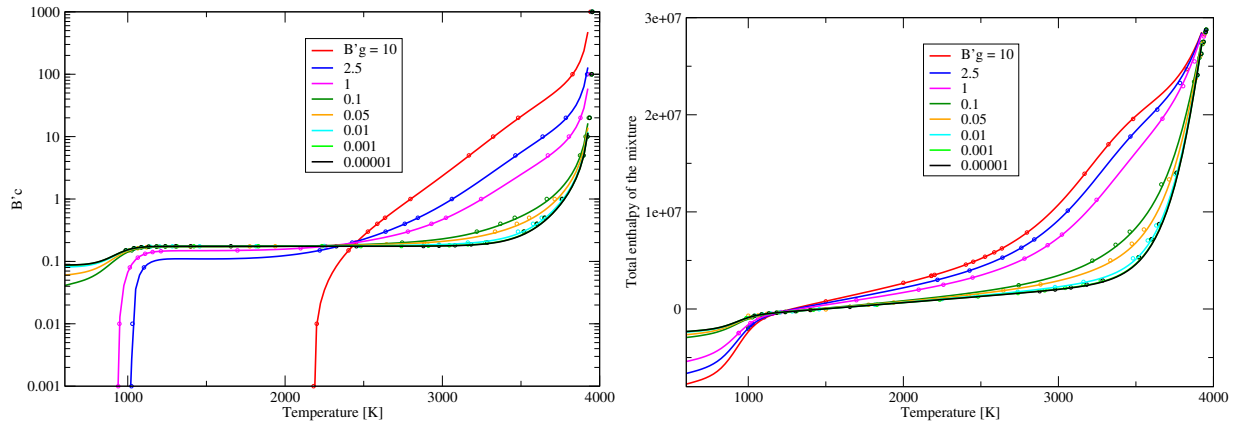
Figure 2. Char rate consumption rate as a function of temperature for a range gas injection rates. The mixture is assumed to be at $p = 1$ atm. The solid lines are from MUTATION-B, the symbols are from MAT.[9]

Figure 2 presents a typical B' table. B'_c is plotted on a logarithmic scale as a function of temperature for a range of pyrolysis-gas injection rates, B'_g. The most noticeable feature is the large plateau over a large temperature range, illustrating the fact that B'_c becomes independent of temperature at low pyrolysis gas injection rate. This illustrates the well known diffusion-limited regime where all of the oxygen transported from the boundary layer edge to the control volume is consumed at the surface. In other words, in this regime, the surface recesses at the same rate independently of the temperature. The gas composition at the wall is plotted in Fig. 3 as a function of temperature for small $\dot{m}_g$. It shows that the gas composition at the surface is independent of temperature in the diffusion-limited regime. At the surface, all of the oxygen available has been consumed by the carbon and is in the form of CO for intermediate temperatures. At lower temperatures, CO_2 is predominant at equilibrium (Boudouard equilibrium); therefore, two moles of oxygen are now necessary to remove one mole of carbon (this corresponds to the lower plateau on the left side of Fig. 2). At very high temperatures, the sublimation regime is observed leading to a sharp increase in the ablation rate.
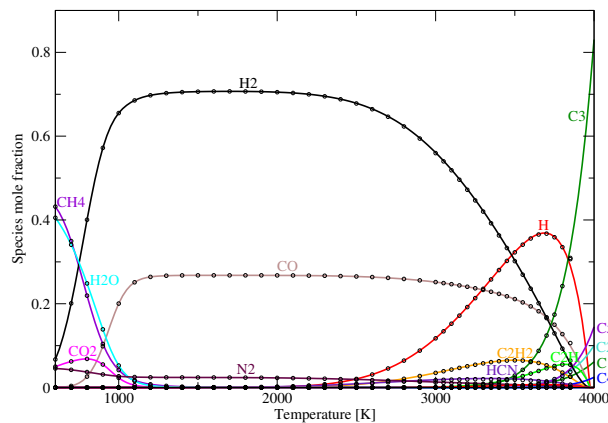
Figure 3. Species mole fractions over temperature for $p = 1atm$ and given $\dot{m}_{pg}$

D. Effects of the thermochemical tables on the B'-tables

A key dataset for accurate estimates of ablation rates is the equilibrium constants needed to compute the equilibrium composition. The equilibrium constants are directly related to the value of the Gibbs free energy

American Institute of Aeronautics and Astronautics

used for each species. At least three different databases are available to compute the Gibbs free energy, g_i, from equations (8) and (14). An option is to use polynomials with coefficients obtained from the CEA[5] or the JANAF[11] thermochemical tables. Another option is to re-compute the Gibbs free energy using a rigid-rotor/harmonic-oscillator approximation based on Gurvich spectroscopic constants.

Figure 4 compares B'-tables computed using the three methods. Significant differences are observed at high temperatures in the sublimation regime. These differences will impact the predictions of material response to high-enthalpy environments.[12] Further work is necessary to analyze and decide on the most appropriate database for use in material response codes. An objective of the present work is to identify the parameters that impact the B'-tables by revisiting the original derivation and identify/verify the approximations used in the formulation.
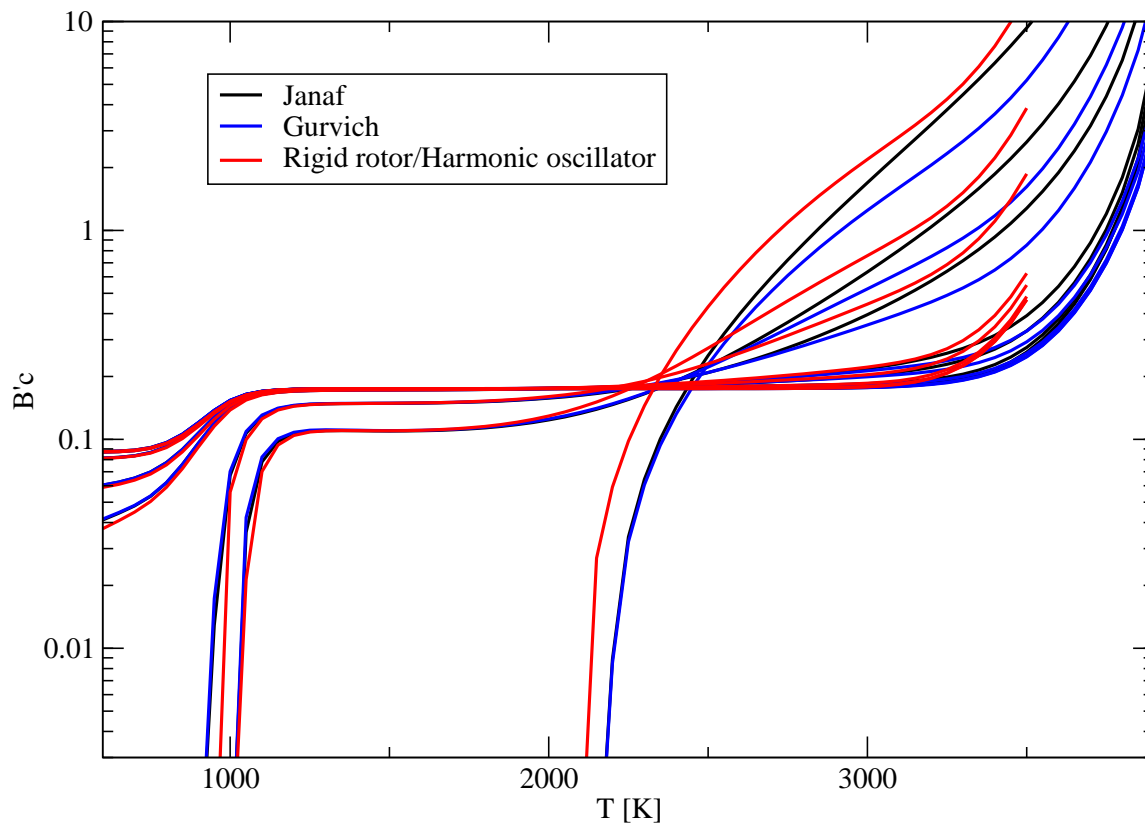
Figure 4. Comparison of Gurvich fit, JANAF fit and Rigid rotor/Harmonic oscillator

III.   Stagnation Line Formulation

A major approximation in the previous B'-tables formulation is reliance on the transfer potential approximation, Eq. 4, to compute the diffusion transport. In the next section, we relax this approximation by solving the Navier-Stokes equations along the stagnation line and compute the species transport. The one-dimensional stagnation line equations are derived in this section from the boundary layer equations in cylindrical geometry. This simplification to the full Navier-Stokes equations enables us to have realistic

American Institute of Aeronautics and Astronautics

chemistry transport models coupled to an equilibrium chemistry approximation at the boundary. We will show that this formulation will provide us with a powerful tool to develop B'-tables.

A.   System of Equations

The governing equations written in conservative form read,

$$\frac{\partial \mathbf{Q}}{\partial t} + \frac{\partial \mathbf{G}(\mathbf{Q})}{\partial x} + \frac{\partial \mathbf{F}(\mathbf{Q})}{\partial y} = \mathbf{S} \tag{19}$$

where $\mathbf{Q}$ is the conservative variable vector, $\mathbf{G}$ and $\mathbf{F}$ are the flux vectors, $\mathbf{S}$ is the source term, x is the coordinate system along the body, and y is along the stagnation line (see Fig.5).
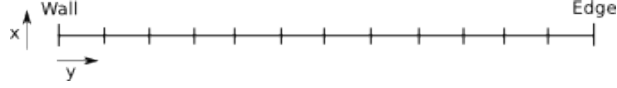
Figure 5.   Coordinate system used where x is along the surface of the body and y is along the stagnation line

Starting with the 2D axisymmetric boundary layer equations,[13] we expand the dependent variables, Q_i, in a Taylor series about the center line, $Q_i(x,y,t) = Q_i(0,y,t) + Q_{i,1}(0,y,t)x + Q_{i,2}(0,y,t)x^2/2 + ...$, where $Q_{i,j} = \partial^j Q_i/\partial x^j$. Substituting the expansion into the boundary layer equations and taking the limit $x \to 0$, we get

$$\frac{\partial}{\partial t}\begin{pmatrix} \rho \\ \rho_i \\ \rho u_{,1} \\ \rho e \end{pmatrix} + \frac{\partial}{\partial y}\begin{pmatrix} \rho v \\ \rho_i v + J_{yi} \\ \rho v u_{,1} - \mu \frac{\partial u_{,1}}{\partial y} \\ \rho v h + \phi \end{pmatrix} = \begin{pmatrix} -2\rho u_{,1} \\ \omega_i - 2\rho_i u_{,1} \\ -\rho u_{,1e}^2 - \rho v_e \frac{\partial u_{,1}}{\partial y}|_e - 3\rho u_{,1}^2 \\ -2\rho u_{,1} h \end{pmatrix} \tag{20}$$

Where v is the velocity along the stagnation line direction y, $u_{,1} = \partial u/\partial x$ is the partial derivative with respect to the wall direction of the velocity in that direction,

$$J_{yi} = -\rho D_{im} \partial y_i/\partial y \tag{21}$$

is the diffusion flux,

$$\phi = -\lambda \partial T/\partial y + \sum_i J_{yi} h_i, \tag{22}$$

is the heat flux, and ρ_i is the mass density of species i. The mixture mass density is given by the expression $\rho = \sum_i \rho_i$. The mixture energy $e = \sum_i y_i e_i$. The mass fraction $y_i = \rho_i/\rho$, mixture enthalpy $h = e + p/\rho$, and pressure $p = \rho R T \sum_i y_i/M_i$, with M_i the molar mass of species i. The production term of species i is given by ω_i.

The properties of the species are computed assuming a rigid rotor and harmonic oscillator approximations; spectroscopic constants are taken from Gurvich.[6] The transport properties are computed following the Chapman-Enskog method. To estimate the viscosity and thermal conductivity, we solve the transport system using the conjugate gradient method. The collision integrals are computed using polynomials from Park.[14] This provide us only with $\Omega^{(1,1)}$ and $\Omega^{(2,2)}$; we have set $\Omega^{(1,2)}$ and $\Omega^{(2,1)}$ to zero. The diffusion fluxes have been computed with the following approximation for Fick's law:

$$D_{im} = \frac{1 - x_i}{\sum_j x_j/\mathcal{D}_{ij}} \tag{23}$$

where $\mathcal{D}_{ij}$ is the binary diffusion coefficient.

B.   Boundary Conditions for the Stagnation line formulation

To complete the system, boundary conditions need to be established for the stagnation line formulation. The boundary conditions of interest for coupling to the control volume formulation are as follows:

American Institute of Aeronautics and Astronautics

Boundary condition at the edge:

At the stagnation line, the height of the boundary layer cannot be defined in terms of the streamwise velocity, and the size of the domain can be arbitrary as long as the assumption of constant pressure holds. Magin[10] defines the edge of the boundary at the stagnation line to be the inflection point of the velocity gradient that is either measured or obtained from a simulation.

At the boundary edge, we specify the species density, $\rho_i|_e$, the normal (to the stagnation line) derivative of the normal velocity, $u_{,1}|_e$, the temperature, T_e, as well as, $\partial u_{,1}/\partial y|_e$. The last term provides information about the shape of the heat-shield in the stagnation line approximation.

The normal velocity at the edge, $v|_e$, is computed by integrating from the wall to the boundary edge using the continuity equation. This insures mass conservation under the constant pressure constraint.

The gas composition at the boundary layer edge, $\rho_i|_e$, is assumed to be in chemical equilibrium. This assumption is valid for large bodies or when the shock is far from the body.

Boundary condition at the wall:

At the wall, the blowing velocity is computed from the relation $v_w = (\dot{m}_{ca} + \dot{m}_{pg})/\rho_w$ and the species mass fraction, $y_i|_w$, is obtained from the *TCV* formulation for a fixed T_w. We set $u_{,1}|_w = 0$, i.e. the pyrolysis gas is injected normal to the wall.

C.   Change of variables

A common problem in reacting flows is that the temperature is needed to compute the properties of the gas, such as the transport coefficients D_{im}, μ, λ, and the production term ω_i, but temperature is not a conserved variable and needs to be derived from the internal energy. In addition, the density, ρ, is computed using the equation of state to ensure that the pressure, p, is constant in the domain. The vector unknown of interest is then: $\mathbf{U} = [v, \rho_i, u_{,1}, T]^T$.

Because the natural unknowns in the integration procedure is the vector of conserved variables $\mathbf{Q} = [\rho, \rho_i, \rho u_{,1}, \rho e]^T$, the following change of variables is required: $\delta \mathbf{Q} = \mathbf{\Gamma} \delta \mathbf{U}$, where $\mathbf{\Gamma} = \partial \mathbf{Q}/\partial \mathbf{U}$. This will lead to a singular matrix, but this has no effect since we are only interested in the steady-state solution. Our equations are written as follows,

$$\mathbf{\Gamma}\frac{\partial \mathbf{U}}{\partial t} + \frac{\partial \mathbf{F}(\mathbf{Q})}{\partial y} = \mathbf{S} \tag{24}$$

D.   Numerical procedure: time and space discretization

The governing equations in conservation law form are solved numerically by means of a finite volume method. The first-order implicit (backward) Euler scheme is use to discretize in time. Second-order differences on a staggered mesh are used to discretize space.[15] The fully discretized equation for cell i at time step n is:

$$A_i \delta U_{i-1} + B_i \delta U_i + C_i \delta U_{i+1} = R_i^n \tag{25}$$

where $\delta U_i = U_i^{n+1} - U_i^n$ and the matrices A_i, B_i, C_i and vector R_i^n are:

$$A_i = -\frac{1}{\Delta y}\left(\frac{\partial F_{i-1/2}}{\partial U_{i-1}}\right)^n \tag{26}$$

$$B_i = \frac{1}{\Delta t}\left(\Gamma_i\right)^n - \left(\frac{\partial S_i}{\partial U_i}\right)^n + \frac{1}{\Delta y}\left(\frac{\partial F_{i+1/2}}{\partial U_i} - \frac{\partial F_{i-1/2}}{\partial U_i}\right)^n \tag{27}$$

$$C_i = \frac{1}{\Delta y}\left(\frac{\partial F_{i+1/2}}{\partial U_{i+1}}\right)^n \tag{28}$$

$$R_i^n = S_i^n - \frac{1}{\Delta y}\left(F_{i+1/2}^n - F_{i-1/2}^n\right) \tag{29}$$

The variables within cell i are coupled to their neighbors $i - 1$ and $i + 1$. Writing Eq. 25 for each cell gives us a block tri-diagonal system which is inverted using the generalized Thomas algorithm. This can be

American Institute of Aeronautics and Astronautics

solved for each δU_i^n so that the solution can be advanced in time: $U_i^{n+1} = U_i^n + \delta U_i$. We note that we are not interested in the time-accurate evolution of the solution, the time dependence being kept only for convergence purposes.

All variables are cell-centered except for v which is computed at the interface (staggered grid) to ensure pressure-velocity coupling at low speed. This would not be possible by means of a preconditioning technique, since p is constant inside the boundary layer.
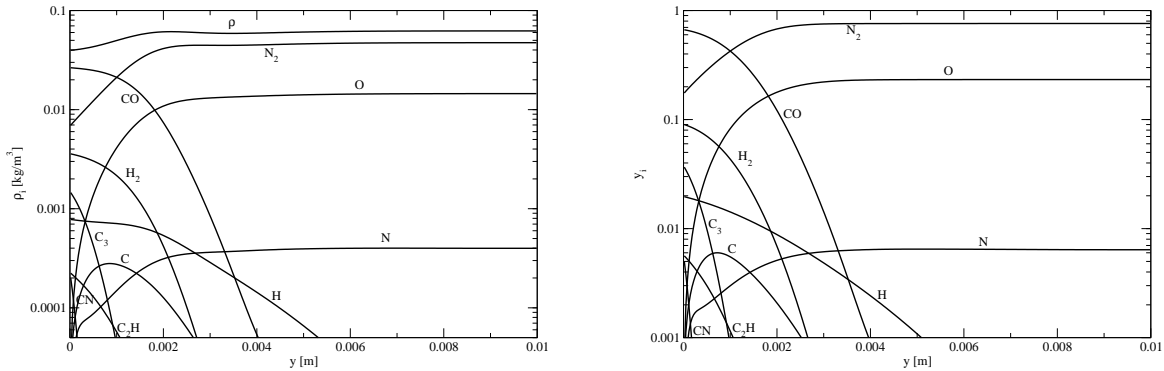
Figure 6. Species-density and mass fraction distribution at the stagnation line of a simulated VKI plasmatron[16] experiment on an ablative carbon-phenolic surface
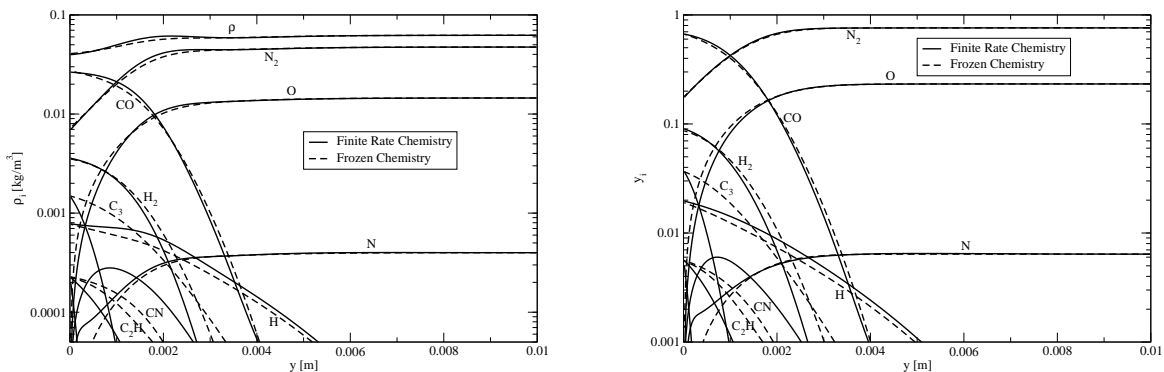
Figure 7. Effects of frozen chemistry compared to finite rate chemistry species-density and mass fraction distribution at the stagnation line of a simulated plasmatron[16] experiment on an ablative carbon-phenolic surface

E. Simulation of an ablating sample in the VKI plasmatron

We have implemented the stagnation-line formulation in a code that we call MUTATION-SL and have verified the implementation by comparing our results to results from the boundary layer code of Barbante.[16] In what follows, we present results for our simulation of the VKI "plasmatron" torch on an ablative material where we have set $p_e = 101325$ [Pa], $T_e = 4640$ [K], $u_{,1e} = 1143[\mathrm{s}^{-1}]$, $u_{,12}|_e = 82069.[\mathrm{m}^{-1}\mathrm{s}^{-1}]$. The wall was set at $T_w = 3200$ [K], with phenol mass injection of $m_{pg} = 0.1$ [Kg m^{-2}s^{-1}]. The velocity at the wall and at the boundary edge were computed to be $v_w = 2.21$ [ms^{-1}] and $v_e = 25.7$ [ms^{-1}] respectively.

Figure 6 shows the species mass fractions as a function of the distance from the wall. At the boundary layer edge we have mostly atomic oxygen and nitrogen entering the boundary layer. Some mass gets convected

American Institute of Aeronautics and Astronautics

as seen in the total density of the N_2 profiles near the wall. It should be noted that it is hard to distinguish between convection and consumption of the species. However, we observe that the atomic species O and N become negligible at the wall. We have oxidation and nitridation as reflected in the profiles of CO and CN. All of the atomic oxygen, O, and atomic nitrogen, N, are consumed at the wall. The main reaction near the wall is the carbon oxidation reaction that produces CO: $C + O \rightarrow CO$. The second important species produced at the wall is hydrogen, H_2.

It observed in non-equilibrium Navier-Stokes simulations that frozen chemistry for air is a good approximation in the boundary layer.[17] In Fig. 7 the composition profiles for frozen chemistry and finite rate chemistry (with and without the reaction term ω_i in Eq. 20) are compared. We find that frozen chemistry holds until the gas from the flow environment start to interact with the gas from the ablation products. We also observe that the slope of the two main species at the wall does not change. This is an indication that the concentrations of CO and H_2 are close to equilibrium, but the minor species, C_3 for example, is not. The implications of active chemistry near the wall may become important at high entry speeds where we expect high temperatures and higher blowing rates.

IV.   Computing B'-tables using the stagnation line formulation

The complete system of equations for the equilibrium boundary condition at the wall is given by Eq. 15; it is repeated here for completeness,

$$
\begin{cases}
\nu_k^k x_k + \sum_j \nu_k^j x_j &= \nu_k^k M y_{k,w}(\dot{m}_{ca})/M_k \\
\sum_i x_i &= 1 \\
-\ln x_C &= \ln K_{C(gr)} \\
\nu_j^j \ln x_j - \sum_k \nu_k^j \ln x_k &= \ln K_j
\end{cases}
\tag{30}
$$

Without the transfer potential approximation, the mass balance at the wall reads,

$$
y_{k,w}(\dot{m}_{ca}) = \frac{\dot{m}_{pg} y_{k,pg} + \dot{m}_{ca} y_{k,ca} - j_{k,w}}{(\dot{m}_{pg} + \dot{m}_{ca})}
\tag{31}
$$

The strategy that we will follow is to compute the species diffusive flux at the wall $j_{k,w} = \sum_i \nu_k^i \frac{M_k}{M_i} J_{yi,w}$ from the stagnation line approximation.

A.   Marching procedure

The boundary layer formulation as well as the TCV formulation require information from each other: the *Stagnation Line* requires v_w, y_{i_w}, and $j_{k,w}$; the TCV formulation requires $j_{k,w}$, as well as $\rho_e u_e C_M$.

To build a B'-table, we need to be able to fix B'_g and vary T_w. Our iteration strategy is shown schematically in Fig. 8,
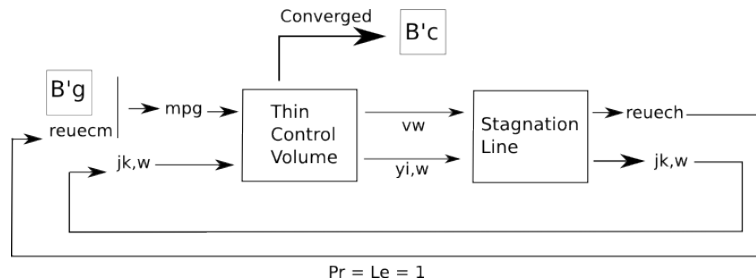
Figure 8. **Marching strategy followed to compute the B'_c give B'_g**

The simplest case to compare the formulation in MUTATION-B with the current formulation is for the case where $Le = Pr = 1$ is assumed to hold. In that case, the B'-table user assumes $\rho_e u_e C_M = \rho_e u_e C_H = \phi_w/(h_e - h_w)$. We start with the stagnation line approximation to compute the cold wall case. This gives us $r_e u_e C_M$. For a given B'_g, we compute $\dot{m}_{pg} = \rho_e u_e C_M B'_g$. Having $\dot{m}_{pg}$, we iterate to compute $y_{k,w}$ and $\dot{m}_{ca}$. Having, values for $\dot{m}_g$ and $\dot{m}_{ca}$, we can compute the velocity at the wall $v_w = (\dot{m}_{ca} + \dot{m}_{pg})/\rho_w$. The

wall conditions are taken as input to the *Flow solver* which in turn gives us a new $\rho_e u_e C_M = \phi_w/(h_e - h_w)$ that needs to be iterated. Once the process has converged, we have $B'_c = \dot{m}_{ca}/\rho_e u_e C_M$. At this point we are ready to move to the next B'_g.

B. Preliminary B'-tables comparison

Because the transport properties are not known for all of the pairs of species present in the mixture that were used to produce Fig. 2, we have reduced the number of species to a set for which all the transport coefficients are available. We reduce the mixture of 19 species that we have discussed previously, to the 11 species set: C, H, O, N, CO, CN, C_2, C_2H, C_3, H_2, N_2.
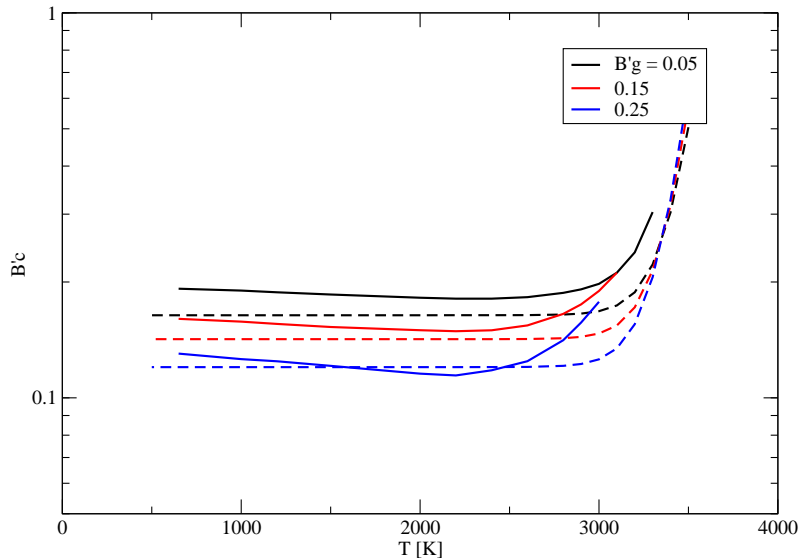
Figure 9. B'_c (char consumption rate) as a function of temperature for a range of B'_g (mass injection rate) rates for $p = 1atm$. The solid lines are from MUTATION-SL, the dashed lines are from MUTATION-B

Figure 9 shows a comparison between the stagnation line formulation in MUTATION-SL, and the formulation in MUTATION-B. We find surprising agreement between the two formulations given that the species profiles (shown in Fig. 6) show little similarity to each other. The B' generated by MUTATION-SL include the effects of blowing. A correction is currently added in the material response code.[18]

Figure 10 compares B'_c profiles computed using frozen chemistry to the profiles generated using finite-rate chemistry. These results are not surprising because we have seen that the effects of chemistry on the profiles of the major species are not strong, and that B'_c, in the diffusion limited regime, is a function of the atomic oxygen and atomic nitrogen supplied to the boundary, and these are the same for the frozen and equilibrium chemistry.

V.   Summary and Conclusions

A stagnation line formulation has been developed to compute the gas surface interactions between an ablating surface and a chemically reactive flow. We find little effect of the treatment of chemistry on the species profiles for the conditions that we have considered. We also find that the frozen chemistry approximation yields reasonable results when compared to treating the chemistry with finite-rate reactions.

The classical *Thin Control Volume* formulation has been implemented in a way that easily couples to a stagnation line approximation (T, p, $\dot{m}_{pg}$ as input, $\dot{m}_{ca}$ as output). A procedure using the stagnation line

American Institute of Aeronautics and Astronautics
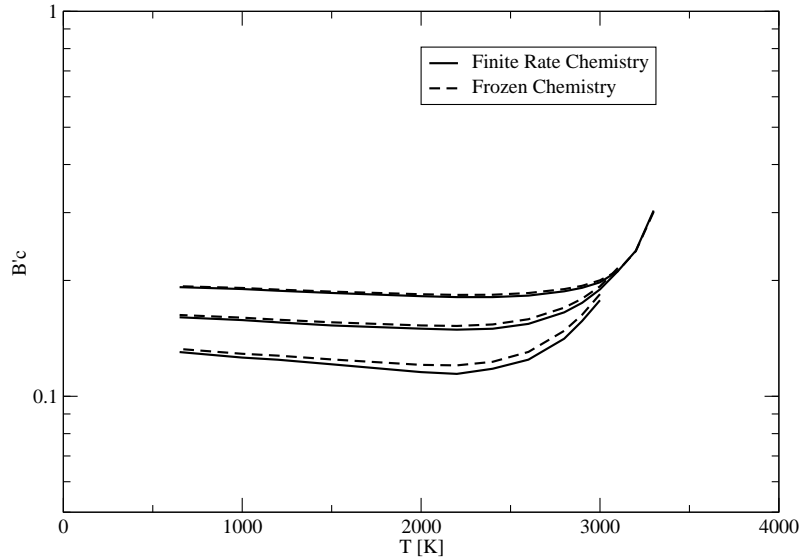
Figure 10. B'_c (char consumption rate) as a function of temperature for a range of B'_g (mass injection rate) rates for $p = 1atm$. Comparison between Finite Rate Chemistry and Frozen Chemistry

approximation has been developed to evaluate the standard approximations used to build B'-tables. The new formulation builds into the B' tables the effects of blowing on the boundary layer transport.

We find that the tables are sensitive to the polynomials used to generate them. But at the conditions tested, the transfer potential approximation seems to hold surprisingly well.

Finally, comparing B'-tables using CEA data, JANAF data, and a rigid-rotor and harmonic-oscillator approximation, we find important differences at high-temperatures.

Acknowledgments

References

[1]KENDALL, R. M., BARLETT, E. P., RINDAL, A. R., AND MOYER, C. B., "An Analysis of the Chemically Reacting Boundary Layer and Charring Ablator. Part V: A General Approach to the Thermochemical Solution of Mixed Equilibrium-Nonequilibrium, Homogeneous or Heterogeneous Systems," *NASA CR-1064*, 1968.

[2]GÖKCEN, T., CHEN, Y.-K., SKOKOVA, K., AND MILOS, F., "Computational Analysis of Arc-Jet Wedge Tests Including Ablation and Shape Change," *AIAA Paper 2010-4644*, 2010.

[3]MACLEAN, M., BARHARDT, M., AND WRIGHT, M., "Implicit Surface Boundary Conditions for Blowing, Equilibrium Composition, and Diffusion-limited Oxidation," *AIAA Paper 2010-1179*, 2010.

[4]GNOFFO, P. A., JOHNSTON, C. O., AND THOMPSON, R. A., "Implementation of Radiation, Ablation, and Free Energy Minimization Modules for Coupled Simulations of Hypersonic Flow," *AIAA 2009-1399*, 2009.

[5]GORDON, S. AND MCBRIDE, B. J., "COMPUTER PROGRAM FOR CALCULATION OF COMPLEX CHEMICAL EQUILIBRIUM COMPOSITIONS AND APPLICATIONS I. ANALYSIS," NASA REFERENCE PUNBLICATION 1311, NASA, 1994.

[6]GURVICH, L. V., VEYTS, I., AND ALCOCK, C., Thermochemical Properties of Individual Substances Fourth Edition.

[7]LACHAUD, J., COZMUTA, I., AND MANSOUR, N. N., "Multiscale Approach to Ablation Modeling of Phenolic Impregnated

American Institute of Aeronautics and Astronautics

Carbon Ablators," *Journal of Spacecraft and Rockets*, Vol. 47, No. 6, NovemberDecember 2010, pp. 910–921.

[8]Lachaud, J., Mansour, N. N., Ceballos, A., Pejakovic, D., Zhang, L., and Marschall, J., "Validation of a volume-averaged fiber-scale model for the oxidation of a carbon-fiber preform," AIAA Paper 2011-2223, 2011.

[9]Milos, F. S. and Chen, Y.-K., "Comprehensive Model for Multi-Component Ablation Thermochemistry," *AIAA Paper 97-0141*, 1997.

[10]Magin, T. E., *A Model for Inductive Plasma Wind Tunnels*, Ph.D. thesis, von Karman Institute for Fluid Dynamics, Universite Libre de Bruxelles, 2004.

[11]Chase, M. W. e. a., "NIST-JANAF Thermochemical Tables (4th ed.)," *Journal of Physical Chemical Reference Data*, Vol. 14, 1985.

[12]Milos, F. S. and Chen, Y.-K., "Ablation Predictions for Carbonaceous Materials Using CEA and JANNAF-Based Species Thermodynamics," *42nd AIAA Thermophysics Conference*, 2011.

[13]Cousteix, J., Aérodynamique - Couche limite laminaire, *Cepadues, 1997.*

[14]Park, C., "Chemical-Kinetic Parameters of Hyperbolic Earth Entry," *Journal of Thermophysics and Heat Transfer*, 2001.

[15]Munafo, A., "Vibrational State to State Kinetics in Expanding and Compressing Nitrogen Flows," *American Institute of Aeronautics and Astronautics*, 2010.

[16]Barbante, P. F., Accurate and Efficient Modelling of High Temperature Nonequilibrium Air Flows, Ph.D. thesis, *von Karman Institute for Fluid Dynamics, 2001.*

[17]Prabhu, D., "Private communication," *ERC/ARC*, 2010.

[18]Chen, Y. K. and Milos, F. S., "Ablation and thermal response program for spacecraft heatshield analysis," *Journal of Spacecraft and Rockets*, Vol. 36, No. 3, 1999, pp. 475–483.